Eur. Phys. J. B **13**, 381–386 (2000)

THE EUROPEAN PHYSICAL JOURNAL B

EDP Sciences

Flame spreading over liquid ethanol

E. Degroote[1,a] and P.L. Garcia-Ybarra[2,b]

[1] EUITA, Dept. Ciencia y Tecnologia Aplicadas (Matematicas), Universidad Politecnica De Madrid, C/ Ciudad Universitaria, s/n 28040 Madrid, Spain
[2] CIEMAT, Dept. Combustibles Fósiles, Av. Complutense 22, 28040 Madrid, Spain

Received 16 October 1998 and Received in final form 23 June 1999

Abstract. Flame spreading over liquid ethanol has been experimentally characterized for ethanol for sub-flash temperatures, in two different channels. Three different spreading regimes have been observed. A uniform region (with flame velocities close to 10 cm/s) appears for values of the initial surface liquid temperature T_∞ above a critical value T_c. For values $T_h < T_\infty < T_c$ an oscillatory regime occurs. For very low temperatures, $T_\infty < T_h$, a new uniform regime appears with slow propagation velocities (close to 1 cm/s). The critical point T_c has been described as a Hopf bifurcation, while T_h resembles a homoclinic connection.

PACS. 47.20.Ky Nonlinearity (including bifurcation theory) – 47.27.-i Turbulent flows, convection, and heat transfer

1 Introduction

Flame spreading is supported by the propagation of a premixed flame existing at the leading edge of the, comparatively, large diffusion flame where most of the vaporized fuel is burned. Many of the flame spreading characteristics are linked to this peculiar flame tip structure, known as triple flame, whose properties have now begun to be understood [1–3]. Moreover, flame spreading over liquid fuels is, in general, also accompanied by liquid fuel motions generated by the Marangoni effect [4]. The non-uniform heating of the liquid fuel under the flame tip produces surface tension gradients that lead to motions in the liquid bulk by viscous stresses. This is a distinctive characteristic with respect to flame spreading above a solid fuel and provides a mechanism to sustain the flame spreading at temperatures well below the flash point temperature T_{fp}. This temperature T_{fp} defines the transition from the gas controlled flame propagation to condensed phase assisted propagation. For higher fuel surface temperatures, the fuel available in the gas phase allows the flame to advance without additional fuel intake from the liquid phase. However, for liquid temperatures lower than T_{fp} the fuel concentration above the liquid lies on the flame extinction region corresponding to the prevailing thermal constraints. Flame propagation is still possible due to the transfer of some extra amount of fuel from the liquid surface, heated locally by the presence of the flame.

For fuel temperatures close to T_{fp}, heat radiation and conduction from the flame are usually the main mechanisms responsible for liquid fuel preheating and a temperature gradient is induced on the liquid surface over a distance of the order of the flame tip size. Only when the induced Marangoni-velocities, corresponding to this temperature gradient, are of the same order of magnitude as the flame spreading velocity does the Marangoni effect become the leading mechanism to drive flame spreading. A vortex-type structure develops ahead of the flame tip that enhances the fuel preheating. The qualitative features of the steady state flame spreading driven by Marangoni effect are described in [5] and a computer code has been developed for this propagation mode [6].

However, both the triple flame and the Marangoni vortex possess very complex structures that have prevented, up to now, the development of a quantitative theory for their coupling. Even more, it is known experimentally [7] that at low enough temperatures, this coupling is unsteady and leads to oscillatory flame spreading. In spite of the work devoted to this phenomenon, the nature of this oscillatory behavior remains controversial and none of the presented models gives a detailed explanation of the mechanisms involved [7–11].

The goal of this research is to shed some light onto this problem by experimentally characterizing the regimes of flame spreading over liquid ethanol when both, liquid and gas, phases are initially at rest, and the surface temperature is kept uniformly constant at some initial value, T_∞, lower than the flash point temperature T_{fp}.

[a] e-mail: edegroote@soc.insetel.es
[b] *Present address*: Escuela Universitaria de Ingeniería Técnica Agrícola, Ciudad Universitaria, s/n. Madrid - 28040, Spain.

2 Experimental setup

To analyze the characteristics of flame spreading over liquid alcohols, we have conducted a series of experiments using an open channel configuration. A long channel of rectangular cross-section, made of duralumin, contains the alcohol. The channel incorporates a refrigerant circuit at the bottom. A liquid coolant flows inside the circuit, coming from a HAAKE-F3 thermal bath. This thermalizing system was able to maintain the temperature in the liquid alcohol uniform along the horizontal, at the beginning of the experiment. The whole channel was covered by a thin metallic net to reduce the influence of air currents on the flame spreading. The net was located 20 cm above the liquid surface. The gas mixture was ignited at one end of the channel and the spreading observed until the flame reached the other end. Two different channels were used. In the first experiment, the channel was 2.5 cm wide, 50 cm long and 4 cm deep, and had two thick Pyrex windows (10 cm length), centered along the lateral walls, one on each side of the container to allow optical access to the fuel layer. Three techniques were used to analyze the flame spreading.

1. Liquid temperatures were measured and controlled by inserting an array of eight Cr-Al thermocouples ($\o 25\mu$) disposed on the fuel surface at regular intervals of 2 cm along the channel (maximum sampling rate was 2 KHz).
2. A classical Teopler schlieren system was used to visualize the large temperature gradients established in the liquid by the intermixing of hot and cold liquid in the Marangoni vortex ahead of the flame, and the pictures through the Pyrex windows were recorded with a video camera recorder (25 frames/s).
3. The spreading of the flame was directly recorded with a video camera from above.

For the lower temperatures, the motion in the liquid ahead of the flame generated an elongated vortex. Thus, the presence of the end wall could affect the results. To improve the data in this region, a new and larger channel was used (the visualization of flame position can be done, in any case, with the video camera records).

This second channel was 100 cm long, 1.5 cm deep and 3.4 cm wide. The direct video recording was confined to the central 65 cm of the channel. The Pyrex windows were eliminated in this second configuration to ensure uniform thermal conditions along the lateral walls. The eight thermocouples were located in the central part along the channel and separated 4 cm from each other. The thermocouples' wires enter laterally from the top towards the bottom of the liquid and after reaching the central part of the channel section, they arrive at the liquid surface from the bottom. In this way only the tips of the thermocouples were located *in the liquid* very close to the surface, reducing then the influence of the wires on flame spreading (the distance between the thermocouples and the liquid surface is approximately 50 μm). Unless otherwise specified, the results given in this paper correspond to experiments carried out on this larger channel. Both channels were filled with ethanol. The voltage generated by the temperature differences between the two Cr-Al welds in the thermocouple was amplified by a factor of 10^3 using a EXP-16 (Metrabyte) amplification card. The data were collected on a PC computer by a DASH-16 (Metrabyte) AD/DA acquisition card.

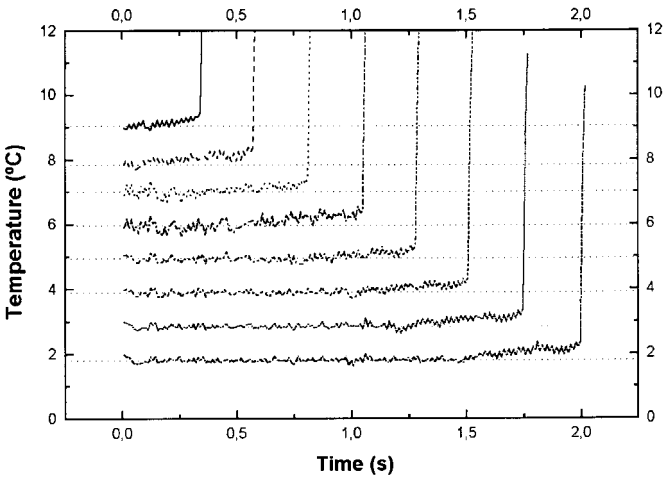

Fig. 1. Detail of the thermocouple reading for $T_\infty = 8.92$ °C The temperature of the thermocouple n has been reduced by $(n-1)$ degrees to avoid the superposition of the lines. Initial time has been arbitrarily chosen.

3 Results and discussion

From the thermocouple readings, the arrival of the flame at each thermocouple location is easily detected. This provides the average spreading velocity between thermocouples (this method of measurement is especially suitable for fast steady propagation regimes due to the high frequency of sampling).

Also, from the direct video recording, a measurement of the spreading velocity, v_f, can be made at any location along the channel. For each video image, we select the geometric line corresponding to the channel's central line. Along this line and after a RGB decomposition (using a color decoder DEC-110-P), only the blue color intensity is digitized with a PC computer ATVista (Truevision) imaging board. The results for successive times are then pasted to obtain a composite image (streak photography). A characteristic composite image is depicted in Figure 2. On this composite image the line separating the dark region (which corresponds to the unburnt side) from the coloured region (which corresponds to the burnt zone) is obtained by enhancing and filtering the image.

The resulting dividing line for the flame spreading of Figure 2 is represented by the dotted line in Figure 6. This line is used to derive the instantaneous flame spreading velocity. Figure 7 depicts the velocity corresponding to the front evolution indicated in Figure 2. After that, the maximum and the minimum spreading velocity of the flame, during the recording interval, can be represented as a function of the initial liquid surface temperature, T_∞.

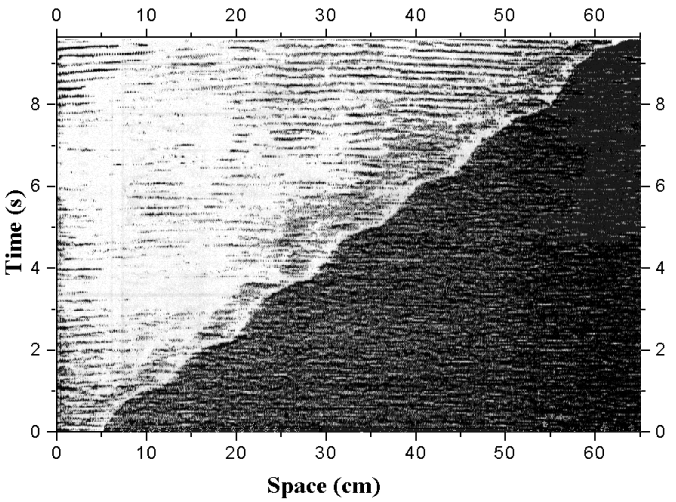

Fig. 2. Streak photography of the channel central line for $T_\infty = -0.5$ °C. Dark zone corresponds to unburnt regions and colored zone to burning regions. The photograph is formed by the superposition of 241 such lines (9.64 s) and covers 730 pixels (65 cm) along the horizontal line.

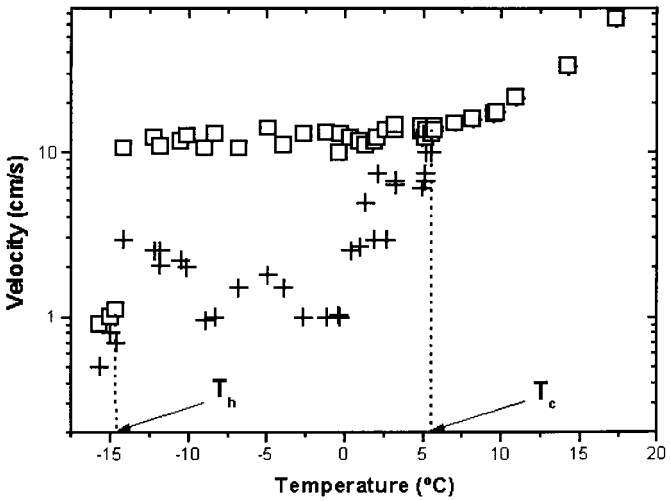

Fig. 3. Bifurcation diagram for the spreading of flames over liquid ethanol for the 100 cm long channel. Squares represent maximum spreading velocities; crosses are the minimum velocities.

The plot of the spreading velocity is depicted in Figure 3. Three different spreading regimes are clearly identified.

3.1 Uniform regime

For temperatures $T_\infty > T_c$, T_c being a first critical value of the system, flame spreading is uniform. Flame velocities vary from $v_{fc} \approx 15$ cm/s (for $T_\infty \approx T_c$) to 65 cm/s (for $T_\infty \approx 17.3$ °C). Figure 1 shows a typical run for uniform flame spreading. The thermocouples record an abrupt increase of the liquid surface temperature, as the flame arrives at the thermocouple location. To appreciate the influence of the flame's relative location on the thermocouple records,the temperatures in Figure 1 have been decreased by $(n-1)$ degrees. Here, n corresponds to the thermocouple number starting with $n = 1$ from the thermocouple which is first reached by the flame. With this temperature shift between thermocouples, we avoid the superposition of the thermocouple readings and are able to appreciate the evolution of the temperature at each location. It is clear, from Figure 1 that the time lag between temperatures increases for consecutive thermocouples (which are located 4 cm apart) is constant, indicating a uniform flame spreading regime.

But even before the abrupt increase in temperature, we can observe that, even for high temperatures, there is a slight increase preceding the flame arrival. This small temperature increase is the indication of the existence of a surface flow; a vortex moving with the flame heats up the fluid well ahead of the flame. An approximated measure of the horizontal length L of this vortex can be made. The results are shown in Figure 4.

The liquid motion is, in this region, restricted to a very thin layer near the surface. In fact, in the shorter channel the lateral Schlieren view of the liquid layer does

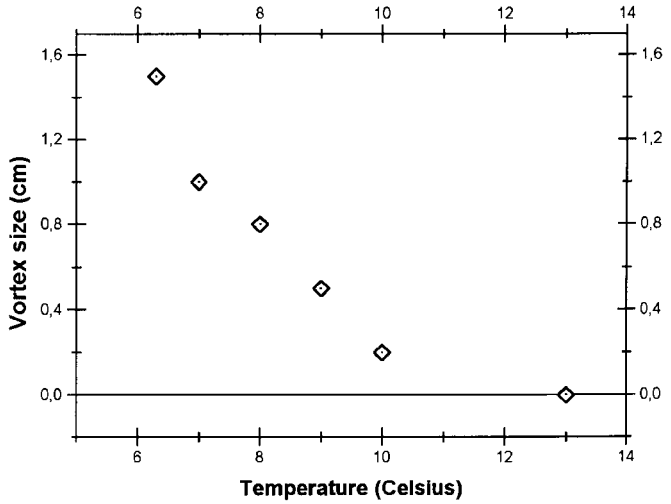

Fig. 4. Approximated horizontal length of the liquid surface motion ahead of the flame *vs.* initial temperature.

not detect clearly the presence of this Marangoni surface motion preceding the flame. The Schlieren image, in the vicinity of the surface, is blackened by the liquid meniscus at the Pyrex windows. The thickness of the region is of the order of a tenth of a centimeter. Therefore the depth of the liquid layer affected by the Marangoni flow should be smaller than the thickness of the liquid meniscus.

Our findings agree with the results reported by Ito *et al.* [10]. By using an interferometric technique, they observed a well developed vortex in this range of uniform spreading.

3.2 Pulsating regime

For temperatures $T_\infty < T_c$, the flame exhibits an oscillatory behavior.

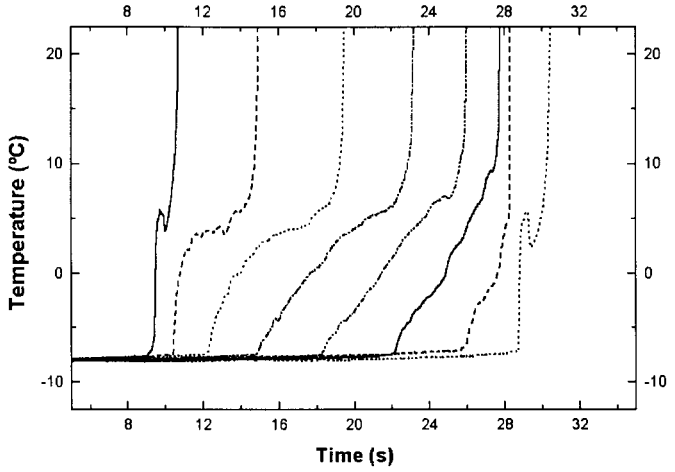

Fig. 5. Temporal evolution of the thermocouples' readings for $T_\infty = -8.0$ °C.

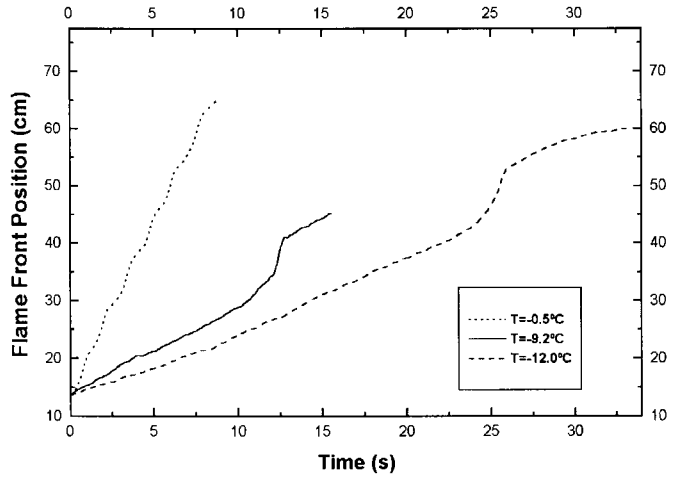

Fig. 6. Evolution of the flame front position for different initial temperatures. Dotted line is for $T_\infty = -0.5$ °C, solid line corresponds to $T_\infty = -9.2$ °C and dashed line is for $T_\infty = -12.0$ °C. Initial time has been arbitrarily chosen for each front.

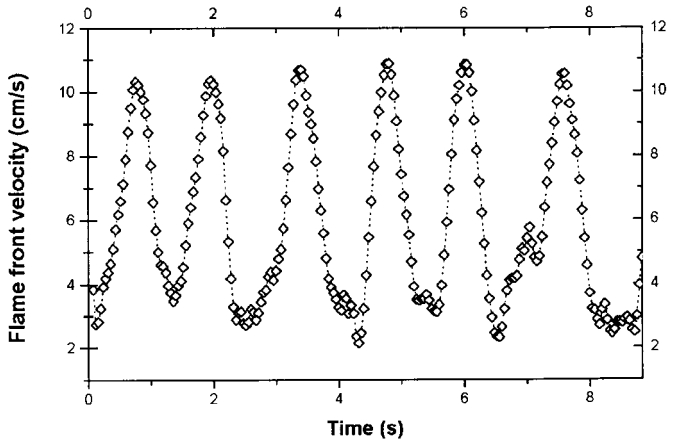

Fig. 7. Temporal evolution of the flame spreading velocity, for $T_\infty = -0.5$ °C, obtained from the dotted line in Figure 6.

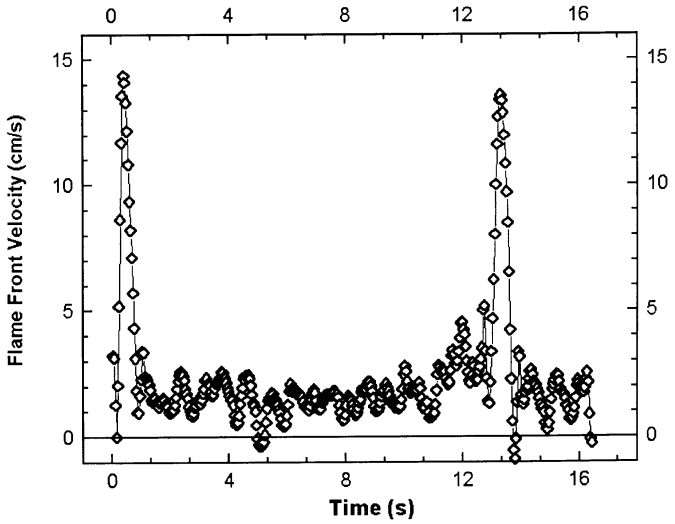

Fig. 8. Temporal evolution of the flame spreading velocity, for $T_\infty = -9.2$ °C, obtained from the solid line in Figure 6.

Comparing the experimental results for both experimental configurations (40 cm channel and 100 cm channel), we can say that the value T_c depends slightly on the channel dimensions, but we cannot conclude any dependence on the channel width for the width range of our channels. The experimental values of T_c are shown in Table 1.

The characteristics of this spreading regime can be enlightened by the response of the thermocouples and the digitized video recordings. The data acquired from the thermocouples presents a time evolution as indicated in Figure 5 (which corresponds to $T_\infty = -8.0$ °C).

The oscillatory spreading starts as a unimodal oscillatory velocity but soon behaves in a more complicated manner. At the beginning of the oscillatory regime, the velocity oscillations are quite regular. Thus, for an initial temperature $T_\infty = -0.5$ °C, Figure 2 depicts the digitized blue color intensity of the channel central line for consecutive times. As we can see in Figure 7, the velocity is always positive and oscillates quite regularly in an unimodal way. For even lower initial temperatures, the behavior of the spreading becomes less regular. Thus, Figure 6 includes also the temporal evolution of the front location for two other initial temperatures, $T_\infty = -9.2$ °C (solid line) and $T_\infty = -12.0$ °C (dashed line). The initial position and time have been chosen arbitrarily on each run. The mean velocity (the mean slope of the curves) decreases with the temperature T_∞. From these plots the corresponding local velocities can be easily obtained.

Figure 8 shows the flame spreading velocity for the solid line in Figure 6 (that is, for $T_\infty = -9.2$ °C). Here, the oscillations become less regular and more than one harmonic appears. Furthermore, for lower temperatures the spreading velocity is small most of the time but presents periodic bursts of rapid propagation. During the oscillatory spreading regime a deeper unsteady vortex is induced in the liquid fuel ahead of the flame. This secondary vortex brings hot liquid from the region under the flame edge

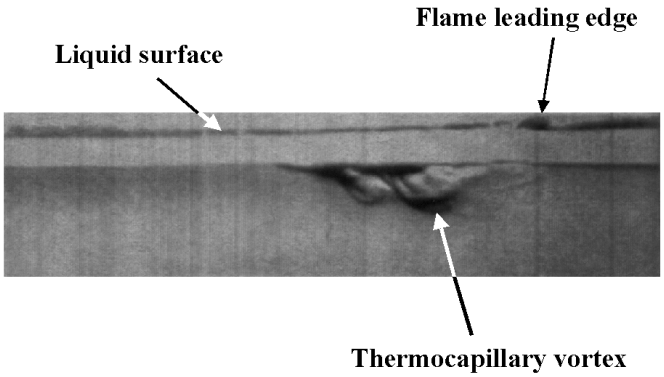

Fig. 9. Image of the recirculating zone in the liquid phase. The image corresponds to the shorter channel, for $T_\infty = -1.2$ °C.

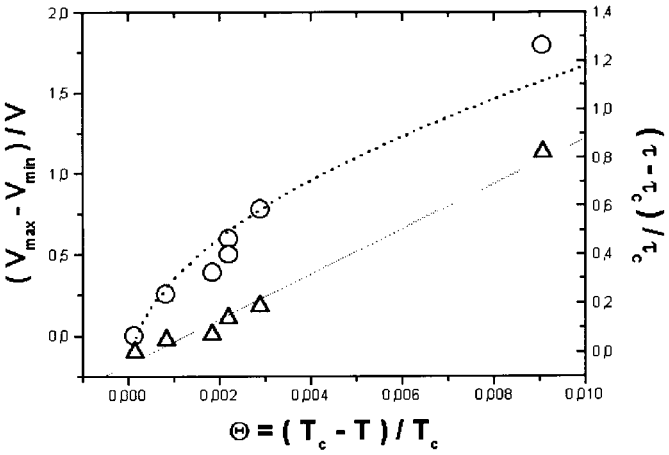

Fig. 10. The amplitude of the pulsating branch (o) and the pulsation period (Δ) around the critical point. Lines are given by equation (1) with $|C_1| = 16.8$; $|C_2| = 87.4$; $T_c = 5.8$ °C; $\tau_c = 0.5$.

and generates a substantial increase of the surface temperature (of the order of 10 degrees) on the affected region. Besides, in the gas phase, another vortex is built up with an enriched (and overhead) reactive gas mixture that assists the combustion process by decreasing the associated chemical reaction time. The oscillatory behavior appears because under these circumstances the flame spreading velocity increases until the vortex structure can no longer follow the flame advancement. Then the flame advances quickly through the enriched gas mixture up to the border of this secondary vortex where the prevailing conditions (leaner and colder mixture) increase the combustion time and retard the advance of the flame. As the flame reduces its propagation velocity, a new recirculating zone is rebuilt in the liquid that, after some induction period, affects the flame by reducing the combustion time. Then the flame accelerates and the process restarts.

The oscillation period has to be identified with the induction time required for the fast propagation burst to occur. The secondary vortex is clearly observed by the schlieren image in the shorter channel. It advances and thickens, attached to the flame, becoming almost 1 cm deep until the burst of rapid spreading overrides it. An example of the Schlieren visualisation is included in Figure 9.

3.2.1 Weakly non-linear pulsations

The value T_c is the threshold at which flame spreading proceeds with an oscillatory velocity. This means that the spreading flame, considered as a dynamic system, has undergone a Hopf bifurcation (see for instance [12]). This kind of transition has universal features that our flame spreading system exhibits: by adopting $T = T_\infty$ as the external control parameter and the amplitude of the oscillatory part of the spreading velocity as an inner variable of the system, theory predicts that, for values *slightly supercritical* of the control parameter and as far as direct bifurcations are concerned, the amplitude of the inner variables and the oscillation frequency have to grow with the separation from the critical point following the laws

$$\frac{v_f^{\max} - v_f^{\min}}{\bar{v}_f} = C_1 \sqrt{\frac{T_c - T}{T_c}}; \frac{\tau_c - \tau}{\tau_c} = C_2 \frac{T_c - T}{T_c} \qquad (1)$$

where the superscripts max and min refer to the maximum and the minimum values of the pulsation velocity, respectively, $\bar{v}_f$ is the average spreading velocity during the pulsation, τ is the oscillation period and C_1, C_2 are constants characterising the system under consideration.

The predictions of these relations have been compared with the experimental results obtained in the long channel. The experimental data are shown to be very well correlated by (1) in Figure 10.

3.3 Pseudo-uniform region

The period of these oscillations is shown in Figure 11 as a function of T_∞. Rhombi correspond to the larger channel and upright crosses to the shorter channel. In fact, in both channels, for surface temperatures $T_\infty < T_h$, the oscillatory spreading disappears and is no longer observed, even for very large periods of time. Instead of the pulsation, a steady flame propagation regime of low velocity (close to 1 cm/s) is observed.

Similar results have been observed for other alcohols. This regime exists for a very significant range of temperature. The critical value T_h does not coincide with the transition to a non-flammable regime; this extinction region (corresponding to values of T_∞ with $v_f < 0$), should correspond to *much lower* temperatures.

Only three measurement points are shown in Figure 3. This fact is a direct consequence of our experimental setup which can not reach lower values of T_∞ because of the thermalizing system. Figure 12 shows the diagram for the shorter channel in this region. A typical response of the thermocouples is given in Figure 13. As can be seen, the eight thermocouples exhibit similar behaviors, with a progressive increase of the surface temperature close to 25 °C.

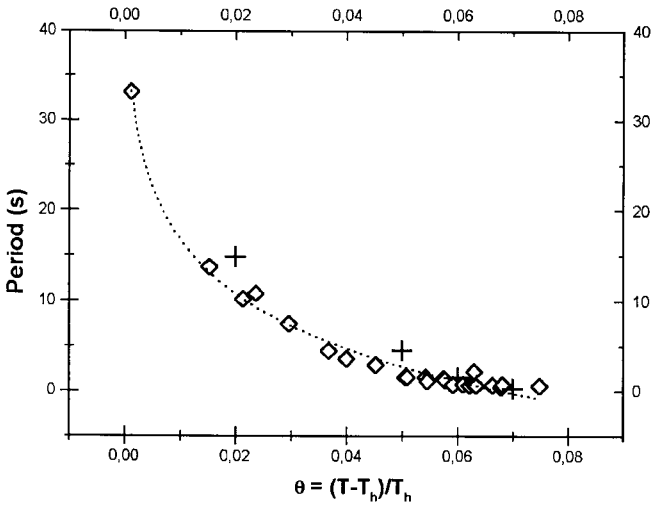

Fig. 11. Periods of flame spreading oscillations *vs.* initial surface temperature.

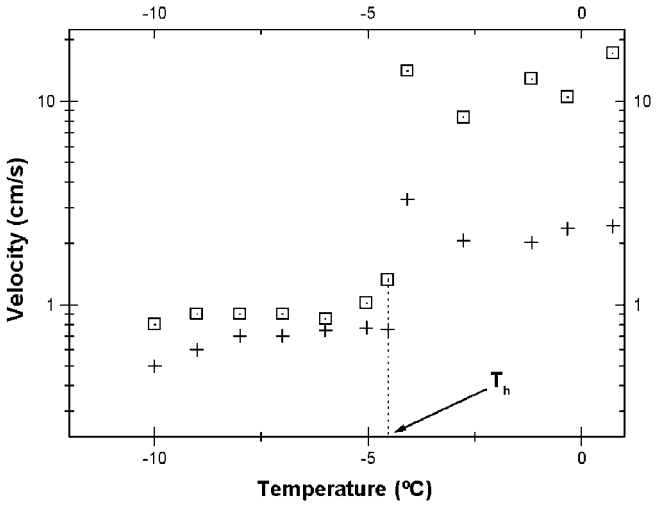

Fig. 12. Bifurcation diagram for the spreading of flames over liquid ethanol for the 40 cm long channel in the low temperature region. Squares represent maximum spreading velocities; crosses are the minimum velocities.

Table 1. Experimental values of $T_{\rm h}$ and $T_{\rm c}$. A strong dependence on the channel dimensions is clearly observed, and may be at the origin of this transition temperature.

	100 cm channel	40 cm channel
$T_{\rm c}$(°C)	5.8	5.3
$T_{\rm h}$(°C)	−14.6	−4.5

The preheated zone appears at each thermocouple location approximately 15 seconds before the flame arrival. Although the horizontal length of this vortex is then of the order of 10 cm, it does not produce the conditions that enable fast flame spreading.

Due to the collision of the limit cycle with that new steady state for $T_\infty = T_{\rm h}$, and due to the divergence of the oscillation period at this point, the transition from the limit cycle to this low velocity regime resembles a homoclinic point. The values of $T_{\rm h}$ for both channels are shown in Table 1. The geometry of the experimental apparatus

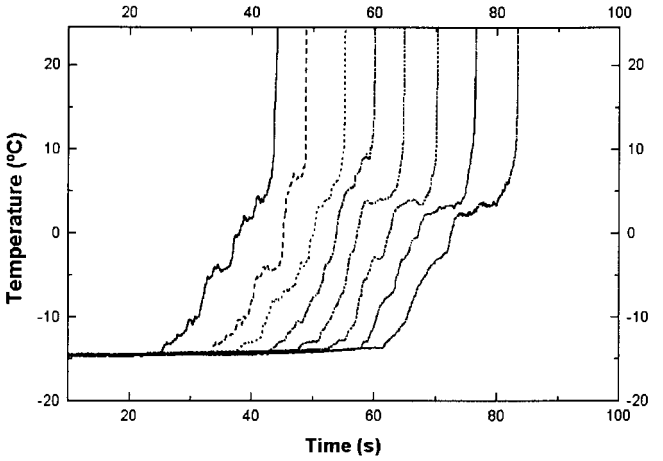

Fig. 13. Detail of the thermocouple reading for $T_\infty = -15.6$ °C for the long channel.

is surely a strong perturbation and may even be at the origin of this transition temperature.

4 Conclusions

The pulsating flame spreading regime over liquid alcohols has been experimentally observed. The oscillation period has been successfully evaluated. Two transition points $T_{\rm c}$, $T_{\rm h}$ have been characterized. The study of the possible influence of the thermal constraints at the lateral boundaries on the flame spreading, and its behavior for different channel dimensions, especially for very low temperatures, can be the subject of future work.

This work has been partially sponsored by the Spanish DGICYT under project number PB94-0385.

References

1. J.W. Dold, Combust. Flame **76**, 71 (1989).
2. A. Liñán, *Combustion in high speed flows, Proceedings of the ICASE Meeting, Oct. 12-14, 1992*, edited by T.L. Jackson, J. Buckmaster and R. Kumar (Kluwer Academic Publisher, 1994), pp. 461-476.
3. P.N. Kioni, B. Rogg, K.N.C. Bray, A. Lian, Combust. Flame **95**, 276 (1993).
4. W.A. Sirignano, I. Glassman, Comb. Sci. Tech. **1**, 307 (1970).
5. F.A. Williams, *Combustion Theory*, 2nd edn. (Benjamin/Cummings Publishers, Menlo Park, CA, 1985).
6. M. Furuta, J. Humphrey, A.C. Fernandez-Pello, Physicochem. Hydrodyn. **6**, 347 (1985).
7. K. Akita, *Fourteenth Symposium (International) on Combustion* (The Combustion Institute, Pittsburgh, 1973), pp. 1075-1083.
8. R. Mackinven, J. Hansel, I. Glassman, Comb. Sci. Tech. **1**, 293 (1970).
9. I. Glassman, F.L. Dryer, Fire Saf. J. **3**, 123 (1980).
10. A. Ito, D. Masuda, K. Saito, Combust. Flame **83**, 375 (1991).
11. C. Di Blasi, S. Crescitelli, G. Russo, *Twenty-Third Symposium (International) on Combustion* (The Combustion Institute, Pittsburgh, 1990), pp. 1669-1675.
12. G. Nicolis, *Introduction to Nonlinear Science* (Cambridge University Press, Cambridge, MA, 1995).